Published in final edited form as:

Cancer Discov. 2017 July ; 7(7): 704–715. doi:10.1158/2159-8290.CD-16-1080.

Phase I Dose Escalation Study of Taselisib (GDC-0032), an Oral PI3K Inhibitor, in Patients with Advanced Solid Tumors

Dejan Juric[1], **Ian Krop**[2], **Ramesh K. Ramanathan**[3], **Timothy R. Wilson**[4], **Joseph A. Ware**[4], **Sandra M. Sanabria Bohorquez**[4], **Heidi M. Savage**[4], **Deepak Sampath**[4], **Laurent Salphati**[4], **Ray S. Lin**[4], **Huan Jin**[4], **Hema Parmar**[4], **Jerry Y. Hsu**[4], **Daniel D. Von Hoff**[5], and **Jose Baselga**[6]

[1]Massachusetts General Hospital Cancer Center, Boston, MA

[2]Dana-Farber Cancer Institute, Boston, MA

[3]Mayo Clinic, Scottsdale, AZ

[4]Genentech, Inc., South San Francisco, CA, USA

[5]Virginia G. Piper Cancer Center Honor Health, Scottsdale, AZ

[6]Memorial Sloan Kettering Cancer Center, New York, NY

Abstract

Taselisib is a potent and selective tumor growth inhibitor through PI3K pathway suppression. Thirty-four patients with locally advanced or metastatic solid tumors were treated (phase I study, modified 3+3 dose escalation; 5 cohorts; 3-16 mg taselisib once daily capsule). Taselisib pharmacokinetics were dose-proportional; mean half-life was 40 hours. Frequent dose-dependent, treatment-related adverse events included diarrhea, hyperglycemia, decreased appetite, nausea, rash, stomatitis, and vomiting. At 12 and 16 mg dose levels, dose limiting toxicities (DLT) were observed, with an accumulation of higher-grade adverse events after the cycle 1 DLT assessment window. Pharmacodynamic findings showed pathway inhibition at ≥3 mg in patient tumor samples, consistent with preclinical *PIK3CA*-mutant tumor xenograft models. Confirmed response rate was 36% for *PIK3CA*-mutant tumor patients with measurable disease (5/14: 4 breast cancer, [3 patients at 12 mg]; 1 NSCLC) where responses started at 3 mg, and 0% in patients with tumors without known *PIK3CA* hotspot mutations (0/15).

Keywords

Taselisib; GDC-0032; PIK3CA; PI3K inhibitor; clinical trial; solid tumors

Corresponding Author: Jose Baselga, MD. PhD, Memorial Sloan-Kettering Cancer Center, Memorial Hospital, New York, NY, USA, baselgaj@mskcc.org, Phone: 212-639-8000, Fax: 212-794-3182.

Conflicts of interest: D. Juric and J. Baselga have no conflicts of interest to declare;

Introduction

In the three decades since the discovery of phosphatidylinositol-3-kinase (PI3K), the connection between cancer and PI3K has been substantiated (1). PI3K catalyzes the transformation of phosphatidylinositol-4,5-bisphosphate (PIP2) to phosphatidylinositol-3,4,5-tripphosphate (PIP3), involved in the phosphorylation of protein kinase B (AKT) and associated proteins in the AKT-mammalian target of rapamycin (mTOR) pathway (2-4). Under normal physiological conditions, the PI3K/AKT/mTOR pathway plays a central role in multiple cellular functions including angiogenesis, proliferation, survival, and metabolism. However, this same pathway turns tumorigenic through the accumulation of genetic aberrations in one or more of several key players, including those in the PI3K family kinase isomers. Among the PI3K family kinase isomers, the class I PI3K isomers are differentiated by their catalytic subunits: p110α, p110β, p110γ, or p110δ. Expression of the PI3Kα isoform can become deregulated through activating mutations or amplifications of the *PIK3CA* gene that encodes p110α. This has been established in several solid tumors, and with an especially high prevalence in cervical cancer (69%), squamous cell lung cancer (53%), head and neck cancer (32%), breast cancer (27%), and endometrial cancer (24%) (5).

Taselisib or GDC-0032 (Genentech, Inc., South San Francisco, CA) is a potent and selective PI3K inhibitor that displays greater sensitivity for mutant PI3Kα isoforms than wild-type PI3Kα (6). Taselisib blocks the PI3K pathway by targeting the ATP-binding pocket in the catalytic subunit of PI3K, leading to inhibition of downstream signaling events, such as those regulating tumor cell proliferation and apoptosis. Taselisib has demonstrated excellent bioavailability with low drug-drug interaction potential (7-9). Our objectives for the current study was to investigate the safety and tolerability of escalating doses of taselisib, as well as early clinical activity in patients with locally advanced or metastatic solid tumors.

Results

Predicting optimal dose from a PIK3CA mutant breast model

Nonclinical studies had demonstrated that taselisib inhibited proliferation of p110α mutant breast cell lines with an average IC_{50} of 70 nM, and inhibited tumor growth in human breast cancer xenograft models harboring *PIK3CA* mutations (6). We conducted additional studies on growth inhibition in a *PIK3CA* mutant breast cancer model to further assist in the identification of the optimal dose and schedule of taselisib in the phase I study. In nude mice bearing KPL-4 breast cancer xenografts that harbor a hot-spot mutation (H1047R) in *PIK3CA*, daily (QD) oral dosing of taselisib at 0.20, 0.39, 0.78, 1.56, 6.25, and 25 mg/kg resulted in dose-dependent tumor growth inhibition and regressions (Fig. 1). Tumor volume traces of individual animals in each cohort confirmed minimum variability in tumor growth inhibition and response (Supplementary Fig. S1). Taselisib was well tolerated with <10% body weight loss in tumor-bearing mice (data not shown). Moreover, robust PI3K pathway suppression in KPL-4 xenografts based on a significant reduction in levels of phosphorylated Akt (Supplementary Fig. S2A), PRAS40 (Supplementary Fig. S2B), and S6 ribosomal protein (Supplementary Fig. S2C) was observed following a single dose of taselisib when compared to vehicle treated animals. Notably, suppression of the PI3K pathway in KPL-4

xenografts for up to 24 hours was observed following a single dose of 25 mg/kg taselisib, and was required for maximum efficacy (Supplementary Fig. S2A-C). The dose-dependent tumor growth inhibition observed in the KPL-4 model (Fig. 1) was used to estimate the taselisib dose expected to lead to efficacy against human tumors. The method utilized was previously described with the PI3K inhibitors, pictilisib (GDC-0941) and apitolisib (GDC-0980) (10, 11). The method combines pharmacokinetics/pharmacodynamics (PK/PD) modeling of the mouse efficacy data with the predicted human PK parameters (12). The predicted dose in human corresponding to the xenograft target tumor growth inhibition of 60%, as proposed by Wong et al. (13), was predicted to be 6 mg daily.

Phase Ia Clinical Trial Design

Dose escalation started at the 3 mg dose level and escalated up to 16 mg before testing of the final cohort at 12 mg (Fig. 2A-B) via a modified 3+3 design. Additional patients were evaluated in certain cohorts in order to replace dose limiting toxicity (DLT) non-evaluable patients (e.g. due to disease progression) and to obtain additional safety data.

Baseline Patient Demographics and Disease Characteristics

From March 2011 to August 2012, 34 patients were enrolled at 3 sites in the United States. The cutoff date for analysis was July 30th, 2014. The median treatment duration was 2 months (range 0.03-15.67). Patients were representative of a heavily pretreated population with a median number of prior therapies of 4 (range 2-13). Further details on the baseline demographics and disease characteristics are shown in Supplementary Table S1.

Safety

Adverse events (AEs) observed with taselisib treatment were consistent with those observed with other PI3K inhibitors, including hyperglycemia, diarrhea, rash, and stomatitis (14, 15). No treatment-related grade ≥3 AEs were observed at the 3, 5, or 8 mg dose levels, so the next dose level tested was the 16 mg dose level. Two of 11 patients treated at 16 mg QD experienced AEs that qualified as a DLT. The first DLT was grade 4 hyperglycemia in a 63-year-old female with pancreatic cancer. The patient was admitted to the hospital on study day 14 and treated with pioglitazone, insulin, and saline hydration, and study drug was permanently discontinued. The event resolved the following day (study day 15). Although it is unclear whether the patient's pancreatic cancer may have caused the patient to be more susceptible to hyperglycemia, this grade 4 hyperglycemia event was deemed a DLT per investigator. The second DLT was grade 3 fatigue in a 65-year-old female with breast cancer on study day 18. Dosing with study drug was held; the event resolved on study day 28.

Although the patient did have some concurrent diarrhea, the grade 3 fatigue was deemed a DLT per protocol definition. While the 16 mg dose level did not technically exceed the maximal tolerated dose (<33% of evaluable patients experiencing DLT), the high frequency of severe AEs that began after cycle 1 (days 1-35) made the 16 mg dose level not tolerable (Supplementary Table S2), and the next dose level tested was at a lower dose of 12 mg. One of 10 patients treated at the 12 mg dose level experienced an AE that qualified as a DLT. This patient had grade 3 acute renal failure secondary to concurrent grade 3 hyperglycemia. The acute renal failure resolved upon discontinuation of study drug and supportive care to

treat the hyperglycemia. Of note, greater than 6 patients were evaluated at the 12 mg and 16 mg cohorts in order to replace DLT non-evaluable patients (e.g. due to disease progression or patients not receiving adequate number of taselisib doses in the DLT window in cycle 1 to be evaluable) and to obtain additional safety data.

AEs related to taselisib, of any grade, were observed in 31 patients (91%), and of grade ≥3 in 14 patients (41%) (Table 1). Grade ≥3 AEs that occurred at a frequency greater than 5% included hyperglycemia (15%), rash (12%), diarrhea (6%), fatigue (6%), and pruritus (6%). Other grade ≥3 AEs observed in one patient included colitis (confirmed via colonoscopy), pneumonitis, lung infection, acute renal failure, skin exfoliation, and stomatitis. The only treatment-related grade ≥4 AE was hyperglycemia as described above. AEs regardless of attribution are provided in Supplementary Table S3 and Supplementary Table S4.

AEs related to taselisib were monitorable, manageable, and reversible. AEs of rash, colitis, and pneumonitis resolved upon holding study drug medication and administration of topical and/or systemic corticosteroids. The grade 3 colitis AE observed had a later onset and occurred on day 160 of treatment. This colitis event resolved upon holding study drug and treatment with corticosteroids. The grade 3 pneumonitis event occurred on day 66 of study treatment; study drug was held and the AE resolved upon treatment with corticosteroids. Hyperglycemia improved upon holding of study drug and/or addition of anti-hyperglycemic medication such as metformin. Such management guidelines were provided for investigators in the protocol.

Although the 12 mg dose level also did not exceed the MTD, the high frequency of grade ≥3 AEs that also occurred after cycle 1 (days 1-35) also gave evidence that this dose level would not be tolerable for future single-agent studies (Supplementary Table S2). For example, treatment-related grade ≥3 AEs at the 12 mg dose level that occurred after cycle 1 included rash (30%), colitis (10%), and stomatitis (10%). Based upon the safety information obtained in this dose escalation and the transition of taselisib to 3 mg capsules, the recommended dose for single-agent taselisib in future studies was 9 mg, daily. A detailed schematic showing the decision-making process for the final dose selection is included in Supplementary Figure S3.

Pharmacokinetics

The group mean time profiles and the dose proportionality for taselisib following single and multiple daily oral doses in cycle 1 and summary of PK parameters are presented (Table 2, Supplementary Fig. S4A-D). After a single dose, the cohort mean half-life ($t_{1/2}$) ranged from 36.7 to 43.8 hr with mean $T_{1/2}$ of ~ 40 hours. The apparent clearance (CL/F) ranged from 4750 to 9170 mL/hr. After 8 daily doses, the apparent clearance at steady state (CL_{ss}/F) ranged from 4320 to 9150 mL/hr. Taselisib exposures, as measured by C_{max} and $AUC_{0\text{-}24}$, were approximately dose proportional with a 2- to 4-fold accumulation and moderate variability in C_{max} and $AUC_{0\text{-}24}$. No apparent time-dependent PK exposure was observed.

Pharmacodynamic modulation of the PI3K pathway

Decreased FDG uptake in tumor sites, consistent with pharmacodynamic modulation of glucose metabolism, has been observed in other trials with PI3K inhibitors and is considered

to be a pharmacodynamic marker of PI3K inhibition given the important role that PI3K plays in cellular glucose uptake (14, 15). Partial metabolic responses (PMRs) with FDG-PET imaging were observed in 70% of patients (16/23 evaluable patients), including at the lowest dose tested of 3 mg QD (Fig. 3). There is a trend of a dose-response, but the small number of patients per dose level does not provide sufficient data to be conclusive. PMRs were observed across multiple tumor types including lung, breast, head and neck, ovarian, endometrial, and adnexal cancers. PMRs were observed in patients with both *PIK3CA* mutant (82%; 9 out of 11) and without known activating *PIK3CA* hotspot mutations (66%; 7 out of 11) tumors (Fig. 4A-C).

Fresh paired tumor biopsies were obtained from 5 patients enrolled onto study that were fixed in optimal cutting temperature (OCT) compound. Of the 5 paired biopsies, 2 non-small cell lung cancer (NSCLC) patients had tumor content in both the pre-treatment and on-study biopsies, and were evaluated by reverse phase protein array (RPPA) for PI3K pathway pharmacodynamic markers, including phospho-Akt (Fig. 5A-B). Decreases greater than 60% in pAKT and pS6 (compared with baseline biopsies) were demonstrated in these patients who were treated with taselisib at doses of 3 mg and 16 mg once daily, respectively.

As inhibition of the PI3K alpha isoform is thought to alter glucose metabolism and result in hyperglycemia, the observation of increased frequency and severity of hyperglycemia at higher doses of taselisib is also supportive of significant inhibition of the PI3K pathway.

Biomarker Profiling of Patient Tumors

Tumor tissue and/or plasma were available from 30 and 33 of the 34 enrolled patients, respectively, for determination of *PIK3CA* mutation status. Fifteen of 34 patients were identified as having *PIK3CA*-mutant tumors, including 13/15 who were classified as *PIK3CA*-mutant based on tissue, with 3 patients also harboring a *KRAS* mutation. One CRC patient harbored both an *AKT1* and *KRAS* mutation. Circulating tumor DNA (ctDNA) analysis from plasma identified the other 2/15 patients with *PIK3CA*-mutant tumors: for one, tumor tissue was without known activating *PIK3CA* hotspot mutations; for the other, no tissue was available. The tissue wild-type, plasma-positive *PIK3CA*-mutant patient was a HER2+ metastatic breast cancer (MBC) patient; tissue and plasma samples were collected ~11 months apart. Two patients had complete loss of PTEN, and 3 were classed as PTEN-low (defined in Methods). Two of the PTEN-low tumors also contained a co-existing *PIK3CA* mutation.

Tumor Responses observed with taselisib treatment

Thirty-two out of 34 enrolled patients had baseline measurable disease. Of the 32 patients, 14 had *PIK3CA*-mutant tumors, 15 had tumors negative for the *PIK3CA* mutations, and the status was unknown for 3 patients. For the 29 patients with known *PIK3CA* mutation status, tumor response evaluation by FDG-PET was available for 23 patients (Fig. 4A) and by radiographic measurements (SLD) for 28 patients (Fig. 4B); the corresponding genetic profiles of the 28 patients with SLD data are presented (Fig. 4C).

The RECIST confirmed response rate was 36% for those with *PIK3CA*-mutant tumors (5/14), and 0% in patients without known activating *PIK3CA* hotspot mutations (0/15). Of

the 5 patients who responded, 4 had breast cancer and 1 had NSCLC with duration of objective response lasting 5.2 months (range 2.8-13.5). Of the 5 patients with confirmed partial responses, all had tumors with mutations in the kinase domain (residue H1047) in the *PIK3CA* gene (Fig. 4). Confirmed partial responses were observed at doses including 3 mg [(n=1; NSCLC, H1047(L/Y)], 5 mg (n=1; breast, H1047R), and 12 mg (n=3; all breast cancer patients with H1047R). While no confirmed partial responses were observed in the 4 patients with helical domain *PIK3CA* mutations, 1 breast cancer patient had an unconfirmed response (-30.52% change from baseline), and 2 patients had tumor shrinkage (-11.41% and -19.98% change from baseline). The fourth patient was a colorectal cancer patient with a concurrent *KRAS* mutation who had progressive disease as his/her best response. In total, we enrolled 6 patients that had a *KRAS* hotspot mutation detected in either tumor tissue or ctDNA. For these 6 patients, 2 had a concurrent *PIK3CA* mutation and 4 had an undetectable *PIK3CA* mutation. Four of the 6 patients with *KRAS* mutant tumors experienced progressive disease as their best clinical response, and 2 patients with *KRAS mutant tumors* experienced stable disease as their best clinical response. Of the 2 patients whose tumor was PTEN-null, both patients experienced progressive disease as their best clinical response.

Four out of 5 patients with a tumor confirmed partial response demonstrated a PMR via FDG-PET (Fig. 4). FDG-PET data was not available for the fifth patient. Several patients had prolonged clinical benefit with the time on study ranging up to 16 months. A detailed swimlane plot showing the duration of treatment for patients via *PIK3CA* mutation status and dose level is also included (Supplementary Figure S5).

Examples of Tumor Responses in PIK3CA-Mutant Breast Cancer Patients

Partial metabolic responses via FDG-PET (Fig. 4) and confirmed partial responses via RECIST (Fig. 4) established promising antitumor activity in patients with *PIK3CA*-mutant breast cancer. Two of the breast cancer patients with confirmed partial responses, highlighted in Supplementary Figure S6A-B, demonstrated shrinkage of lesions in visceral organs such as the liver.

Although longitudinal, on-study ctDNA collections were not mandatory in this study, a total of 4 collections from a HR+, HER2- metastatic breast cancer patient who was treated at the 12 mg dose level and experienced a confirmed partial response on taselisib were taken. The data demonstrated the changes in *PIK3CA* mutant allele frequencies over time for this specific patient and showed a correlation of a decrease of *PIK3CA* mutant allele frequency with the partial response, and subsequent increase upon disease progression at day 466, albeit in a single patient (Supplementary Figure S7).

Discussion

Taselisib was dosed in patients from 3-16 mg, administered once daily. One of 10 patients treated at 12 mg and 2 of 11 patients treated at 16 mg experienced AEs that qualified as DLTs. Although 16 mg did not exceed the MTD as defined by DLTs in cycle 1, no higher dose beyond 16 mg was tested based upon the overall tolerability of taselisib that included

assessment of the frequency/severity of AEs outside of the DLT window. Patients treated at the higher doses (12-16 mg) experienced increased frequency of fatigue and hyperglycemia.

The overall AE profile for taselisib in the current study was largely consistent with other PI3K inhibitors (14-16). Buparlisib (BKM120), a pan-class inhibitor that targets all 4 isomers of PI3K, had rash, hyperglycemia, diarrhea, and mucositis as frequent treatment-related AEs (14). In-class toxicities for pictilisib, another pan-class PI3K inhibitor, included diarrhea, hyperglycemia, rash, and pneumonitis (15). Colitis observed with taselisib is similar to that reported with idelalisib, a PI3K delta isoform-specific inhibitor approved for the treatment of hematologic malignancies (17), and is associated with a delayed onset diarrhea that requires systemic corticosteroid treatment. Therefore, taselisib data are consistent with a possible mechanism of PI3K delta isoform inhibition being involved in colonic inflammation. With pneumonitis, however, it is unclear as to which PI3K isoform is responsible for the AE, for pneumonitis has been observed in patients treated with pan-class I inhibitors and with taselisib (14-16).

Taselisib was rapidly absorbed (T_{max} 2-4 hours) and demonstrated dose-linear and time-independent PK with moderate PK variability. The single dose half-life was approximately 40 hours, enabling daily dosing with adequate drug exposure to suppress the PI3K signaling pathway. Evidence of pharmacodynamic target inhibition was observed in paired tumor biopsies as assessed by RPPA analysis of key signaling markers downstream of PI3K. We also observed decreased expression of phospho-ERK from paired tumor pharmacodynamics biopsies. One potential explanation relates to feedback inhibition observed in oncogenic signaling pathways. Inhibition of PI3K signaling has been shown to activate MAP-kinase signaling at early time-points through receptor tyrosine kinase activation (18, 19). However, sustained MAP-kinase activation has also been shown to negatively regulate phospho-ERK activity through DUSPs in receptor tyrosine kinase activated cells (20). Interestingly, the 2 tumor biopsies analyzed in this study were non-small cell lung cancer tumors, one of which contained an activating *EGFR* exon 19 deletion mutation. FDG-PET responses were also observed in patients, consistent with PI3K-dependent inhibition of glucose metabolism.

Pharmacodynamic modulation as shown by FDG-PET responses and paired tumor biopsies occurred in the first cohort tested at the 3 mg dose level, consistent with robust inhibition of the PI3K pathway. While preclinical experiments have predicted that an exposure corresponding to the 6 mg dose level would be the minimal efficacious dose, in this phase Ia trial, we observed antitumor activity and PI3K pathway knockdown starting at the 3 mg dose in the first cohort. Four out of 5 patients with tumor partial responses also had FDG-PET responses; the fifth patient did not have FDG-PET data.

Single-agent anti-tumor activity by CT scan was observed in five patients receiving 3-12 mg taselisib. All responses observed were in *PIK3CA*-mutant tumors. Based upon preclinical data, taselisib is expected to be active against tumors with either helical or kinase domain mutations. Confirmed partial responses were observed in patients with *PIK3CA* kinase domain mutations. There were fewer patients enrolled with helical domain mutations (n=4). One breast cancer patient with a helical domain mutation did have an unconfirmed response (E545K), 2 patients had tumor shrinkage, and the fourth patient was a colorectal cancer

patient with a concurrent *KRAS* mutation which may render tumors relatively resistant to PI3K inhibitors. Three of the confirmed partial responses were observed at the 12 mg dose level.

The increased antitumor response in *PIK3CA*-mutant cancer patients in this study as compared to prior PI3K inhibitors tested in the clinic may be due to several factors. One possible reason could be an increased therapeutic index for taselisib in patients with *PIK3CA*-mutant tumors. Taselisib has increased potency against the mutant version of the PI3K alpha isoform, as demonstrated in chemical assays as well as in cancer cell lines (6). A higher therapeutic window due to greater selectivity for PIK3CA mutant isoforms has been shown in extensive laboratory studies (21) and is also suggested by the fact that partial responses were only observed in patients with PIK3CA-mutant tumors. The other indirect evidence for an enhanced therapeutic window is that at the chosen recommended dose, patients were able to stay on the study agent for prolonged periods of time. On the contrary, with pan-PI3K inhibitors, the majority of patients had to discontinue the study agent due to lack of tolerability (22, 23). Of note also, since taselisib inhibits the PI3K beta isoform 30-fold less than the PI3K alpha isoform, the decreased anti-tumor activity against PTEN-null tumors is consistent with the observation that PTEN signals through *PIK3CB* (24). Others reported that acquired resistance to the alpha-selective PI3K inhibitor, alpelisib (BYL-719), can occur through loss of PTEN expression (25). Recent phase I clinical data with alpelisib and letrozole showed increased clinical benefit rate in patients with PIK3CA-mutant tumors (26). We also did not observe any clinical responses in taselisib-treated patients whose tumor contained a *KRAS* mutation. This is consistent with the observation that cell lines harboring somatic alterations in *RAS/RAF* genes are insensitive to the pan-PI3K inhibitor GDC-0941 (27).

Taselisib exhibited a favorable safety profile and early signs of promising activity, especially in tumors that have activating mutations in *PIK3CA*. Further studies as a single agent are ongoing. Given that approximately 40% of estrogen receptor positive (ER+) breast cancers harbor the *PIK3CA* mutation and given the extensive crosstalk between the ER and the PI3K signaling pathways (28), there is a strong rationale to evaluate taselisib in combination with endocrine therapy. Based upon these promising phase Ia data showing antitumor activity in the first cohort tested as well as subsequent phase Ib/II data of taselisib in combination with fulvestrant (29, 30), an ongoing randomized phase III study is testing taselisib plus fulvestrant in postmenopausal women with ER+ metastatic breast cancer with enrollment being enriched for patients with *PIK3CA*-mutant tumors (SANDPIPER; clinicaltrials.gov NCT02340221).

Methods

In-Vivo Efficacy

All in-vivo efficacy and pharmacodynamic studies were approved by Genentech and Institutional Animal Care and Use Committee (IACUC) and adhered to the NIH Guidelines for the Care and Use of Laboratory Animals. Human KPL-4 breast cancer cell line was obtained from J. Kurebayashi (Kawaski Medical School; Kurashiki; Okayama, Japan) in August, 2006. The cell line was established from the malignant pleural effusion of a breast

cancer patient with an inflammatory skin metastasis. Cells were authenticated by short tandem repeat (STR) fingerprinting within 6 months of engraftment into mice for efficacy and pharmcokinetic/pharmacodynamic studies as described. KPL-4 cells, resuspended in 50% phenol red-free Matrigel (Becton Dickinson Bioscience; San Jose, CA) and Hank's Balanced Salt Solution, were inoculated into 100 SCID beige mice (Charles River Laboratory, Wilmington, MA) in the number 2/3 mammary fat pad. Each mouse was injected with 3×10^6 cells. Tumors were monitored until they reached a mean tumor volume of 150-200 mm^3. Tumor volume was measured using Ultra Cal-IV calipers (Model 54-10-111; Fred V.Fowler Co.; Newton, MA). The following formula was used in Excel, version 11.2 to calculate tumor volume: Tumor Volume (mm^3) = (Length × $Width^2$) × 0.5. Mice were distributed into seven groups of 8 mice based on tumor volume with a mean tumor volume across all groups of 171 ± 5.1 mm^3 (mean ± standard deviation of the mean) on day 0 of the study. Taselisib was formulated in a vehicle containing 0.5% methycellulose/ 0.2% Tween-80. Mice were administered 0 (Vehicle) or 0.20, 0.39, 0.78, 1.56, 6.25, and 25 mg/kg GDC-0032 orally (PO) by gavage daily for 21 days in a volume of 100 μL. Tumor sizes were recorded twice weekly over the course of the study. Mouse body weights were also recorded twice weekly. Mice whose tumor volume exceeded 2000 mm^3 or whose body weight loss was 20% of their starting weight were promptly euthanized. A mixed modeling approach was used to analyze the repeated measurement of tumor volumes from the same animals over time (31). This approach addresses both repeated measurements and modest dropouts due to any non-treatment related death of animals before study end. Cubic regression splines were used to fit a non-linear profile to the time courses of $\log_2$ tumor volume at each dose level. These non-linear profiles were then related to dose within the mixed model. Tumor growth inhibition as a percentage of vehicle control (%TGI) was calculated as the percentage of the area under the fitted curve (AUC) for the respective dose group per day in relation to the vehicle, using the following formula: $\%TGI=100 \times (1 - AUC_{dose}/AUC_{vehicle})$.

Pharmacodynamic Marker Analysis in KPL-4 Tumor Xenografts

Human KPL-4 cells, resuspended in 50% phenol red-free Matrigel (Becton Dickinson Bioscience®; San Jose, CA) and Hank's Balanced Salt Solution, were inoculated into 80 SCID beige mice in the number 2/3 mammary fat pad. Each mouse was injected with 3×10^6 cells. Tumors were monitored until they reached a mean tumor volume of 350-400 mm^3 after which mice were treated with a single oral dose of vehicle (0.5% methylcellulose/0.2% Tween-80) or 1, 5 and 25 mg/kg of taselisib for 1, 4, 8, 24 and 48 hours (n=4 tumor-bearing animals for each dose and time-point). Following drug treatment, tumors were harvested, snap-frozen in liquid nitrogen and processed for protein extraction using a buffer (Invitrogen; Camarillo, CA), containing 10 mM Tris pH 7.4,100 mM NaCl, 1 mM EDTA, 1 mM EGTA, 1 mM NaF, 20 mM $Na_4P_2O_7$, 2 mM Na_3VO_4, 1% Triton X-100, 10% glycerol, 0.1% SDS, and 0.5% deoxycholate supplemented with a phosphatase and protease inhibitor cocktail (Sigma, St. Louis, MO). Tumors were dissociated with a small pestle (Konte Glass Company; Vineland, NJ) in extraction buffer, sonicated briefly on ice, and centrifuged at maximum RPM for 20 minutes at 4°C. Protein concentrations were determined using the BCA Protein Assay Kit (Pierce; Rockford, IL). The Meso Scale Discovery Multi-Spot Biomarker Detection System (Meso Scale Discovery; Gaithersburg, MD) was used to

determine the levels of total Akt, Akt phosphorylated at serine 473 (pAkt), total S6RP, and S6RP phosphorylated at serine 235/236 (pS6RP). Total PRAS40 and PRAS40 phosphorylated at threonine 246 (pPRAS40) were detected by ELISA (Invitrogen; Carlsbad, CA). Levels of phosphorylated protein were normalized to total protein levels in taselisib-treated tumors and compared to vehicle-treated controls.

Study Population

This was a phase I, multicenter, open-label modified 3+3 dose-escalation study. The protocol was approved by Institutional Review Boards prior to patient recruitment and conducted in accordance with International Conference on Harmonization (ICH) E6 Guidelines for Good Clinical Practice and Declaration of Helsinki. All patients gave written informed consent and a willingness to provide tumor archival tissue. Patients had histologically documented locally advanced or metastatic solid malignancies that had progressed or failed standard therapy. Other key inclusion criteria included evaluable or measurable disease as defined by RECIST version 1.1 (32), age ≥ 18 years, life expectancy ≥ 12 weeks, ECOG performance status 0-1, adequate hematologic and organ function, and fasting blood glucose level ≤ 120 mg/dL. Key exclusion criteria included type I or II diabetes mellitus requiring anti-hyperglycemic medication, active small or large intestine inflammation, prior treatment with a PI3K inhibitor in which the patient experienced a grade ≥ 3 drug-related AE, primary CNS malignancy or untreated/active CNS metastases, or severe uncontrolled systemic cardiac, lung, or liver disease. A 3-week washout period from any ongoing cancer therapy was required prior to start of taselisib dosing.

Study Design

Cycle 1 (days 1-35) began with a pharmacokinetic (PK) evaluation; patients received a single fasting dose of taselisib on day 1 at their assigned dose level followed by a 7-day washout period in which frequent PK sampling up to 72 hours was performed. Urine samples were collected up to 24 hours. Continuous daily dosing (fasting) resumed on day 8 for 4 weeks. Subsequent cycles were 28 days in length. A modified 3+3 dose escalation scheme was implemented to determine the maximum tolerated dose (MTD) and to identify the recommended dose for future studies. Taselisib administration was discontinued in patients who experienced disease progression or unacceptable toxicity.

Study Treatment

Taselisib (Genentech, Inc.) was taken on an empty stomach as a single dose (powder-in-capsule formulation) at the same time of day +/- 2 hours (33). The dose for each patient was dependent on the dose level assignment.

Safety

Safety was evaluated by incidence, nature, severity, and relatedness of AEs, and graded according to NCI CTCAE v4.0. All AEs regardless of attribution were collected until 30 days following the last administration of treatment or study discontinuation/termination, whichever was later. Dose limiting toxicities (DLTs) were defined as drug-related AEs observed during cycle 1 (days 1-35) and included any grade ≥ 3 non-hematologic toxicity

with exception of grade diarrhea, nausea, or vomiting that responded to standard-of-care therapy. Hematologic toxicities defined as a DLT included grade ≥ 4 thrombocytopenia or grade ≥ 4 neutropenia (absolute neutrophil count < 500/μL) lasting > 5 days or accompanied by fever. Fasting grade ≥ hyperglycemia, fasting grade ≥ 3 hyperglycemia for ≥ 1 week despite adequate trial of oral anti-hyperglycemic therapy, grade ≥ 4 fasting hypercholesterolemia or triglyceridemia for ≥ 2 weeks despite intervention with lipid-lowering agent, or grade ≥ 3 serum bilirubin or hepatic transaminase (alanine aminotransferase or aspartate aminotransferase were considered DLTs. For patients with bone or liver metastases and baseline levels of ≤ 5× upper limit of normal (ULN) hepatic transaminase or alkaline phosphatase, levels of > 10× ULN was considered a DLT. The MTD was defined as the highest dose at which < 33% of patients developed a DLT during the DLT assessment window.

Pharmacokinetics

Taselisib PK was evaluated based on collection of serum samples during cycle 1 at pre-dose, 0.5, 1, 2, 3, 4, 8, 24, 48, and 72 hours post-dose. Additional samples were collected at pre-dose, 2 hours post-dose on day 8 of cycle 1, and pre-dose, 0.5, 1, 2, 3, 4 and 8 hours post-dose on day 15 of cycle 1. Pre-dose and post-dose samples were also collected on days 22 and 29 of cycle 1, then on day 1 of every cycle thereafter. Taselisib concentration was determined using a validated LC-MS/MS analytical procedure (Covance Laboratories, Madison, WI) (34). The lower limit of quantification (LLOQ) was 0.87 nM. The PK assessment from patients was performed for cycle 1 plasma concentration-time data using standard non-compartmental (NCA) PK methods in WinNonlin (Version 5.2.1, Pharsight Corp., Mountain View, CA). The relationship of individual day 1 and steady-state C_{max} and AUC values versus taselisib (GDC-0032) dose was evaluated with a power law model (C_{max} or AUC = a $(Dose)^{power}$) with 95% CI of slope to the pharmacokinetic relationship between dose and taselisib exposure (C_{max} or AUC).

FDG-PET Imaging

To assess the effects of taselisib on tumor metabolism or as a marker of response to therapy, ^{18}F fluorodeoxyglucose (FDG)-positron-emission tomography (PET) scans were obtained at baseline and during the last week of cycle 1 if at least one PET-assessable lesion was observed at baseline. Any significant changes in tumor FDG uptake required a repeat FDG-PET during cycle 2. For PET evaluation, up to 5 target lesions with a target to background uptake level greater or equal to 2 were selected in the screening scan. Target lesions were to measure at least 15 mm in longest diameter (LD) on CT or MRI. In the case there were not 15 mm diameter FDG-avid lesions, lesions of at least 10 mm in LD meeting RECIST 1.0 criteria were selected. An FDG-PET partial metabolic response (PMR) was defined as a decrease of > 20% in the average percentage change in the maximum standardized uptake value (SUV_{max}) of the target lesions.

Reverse Phase Protein Array Analysis of Tumor Biopsies

To assess pharmacodynamic effects on tumor and whether inhibition of PI3K with taselisib resulted in changes in pathway markers, pre- and post-treatment paired tumor biopsies were obtained at baseline and during cycle 1 from patients who provided consent for tissue

biopsy. Tumor samples were assessed for decreased phosphorylation on downstream analytes, such as proline-rich AKT substrate 40 (pPRAS40), phosphorylated extracellular signal-regulated kinase (pERK), and phosphorylated ribosomal protein S6 (pRPS6), using reverse phase protein arrays (RPPA) (Theranostics, Rockville, MD) as previously described (35).

Tumor Assessments

Taselisib activity was evaluated by tumor CT assessments every 8 weeks, with confirmation of objective response ≥ 4 weeks after initial documentation (per RECIST v1.1).

Determination of PIK3CA Mutation Status

A patient was determined to harbor a *PIK3CA* mutant tumor if a positive mutation result was obtained from either tissue or plasma.

Assessment of somatic mutations from tissue—*PIK3CA* mutation hotspot status was assessed centrally using PCR-based platform from DNA extracted from paraffin embedded formalin fixed (FFPE) tissue using PCR-based platforms as described previously (36). *PIK3CA* hotspot coverage included: C420R, E542K, E545A/G/K, H1047L/R/Y. Samples were subsequently molecularly profiled using an internally developed 120 somatic hotspot mutation test (MUT-MAP) that detected somatic mutations in *AKT1, BRAF, EGFR, FGFR3, FLT3, HRAS, KIT, MET, NRAS* and *PIK3CA*, as described previously (37). In addition to the central assessment of the eight *PIK3CA* hotspot mutations, the MUT-MAP somatic mutation test detected an additional nine mutations: *R88Q, N345K, E545D, Q546R/E/K/L, M1043I,* and *G1049R.*

Assessment of somatic mutations from plasma—Circulating tumor DNA (ctDNA) analysis of somatic mutations was determined centrally using the Sysmex Inostics Oncobeam Panel 1 (Hamburg, Germany), which detects hotspot mutations in *AKT1, BRAF, KRAS, NRAS,* and *PIK3CA*. *PIK3CA* hotspot coverage included: *E542K, E545G/K, Q546K, M1043I, and H1047L/R/Y*.

Determination of PTEN status—PTEN status was centrally determined using the Ventana Benchmark XT instrument with standard immunohistochemistry techniques and employing an anti-PTEN antibody (clone 138G6; Cell Signaling Technology). Samples were scored using a H-score methodology using the following equation: H-score = (% × 0)+(% × 1+)+(% × 2+)+(% × 3+)+(% × 4+), where 3+ is the staining intensity of surrounding normal tissue. A PTEN-null tumor was defined as H-score of 0, a PTEN-low tumor was defined a H-score between 1-100, and a PTEN- normal tumor was defined as H-score greater than 100.

Statistical Methods

The sample size for this study was based on the dose escalation rules described in the study design section and was not based on explicit power or type I error considerations. Safety analyses included all patients who received any amount of taselisib. All AEs occurring on or

after treatment on day 1 were summarized by mapped term, appropriate thesaurus levels, and NCI CTCAE v4.0 toxicity grade.

Supplementary Material

Refer to Web version on PubMed Central for supplementary material.

Acknowledgments

The authors wish many thanks to all of the patients and the investigators who participated in this study. We thank M, Negash, M. Grow, and V. Brophy (Roche Molecular Systems, Pleasanton, CA) for development of the *PIK3CA* research mutation test. We also thank members of our Clinical Assays and Technologies Group for running the MUT-MAP mutation test, Y. Yan and M. Wagle for help with the RPPA assay, S. Carroll, J. Aimi, and J. Shine for sample logistics, and J. Qiu and V. Ng for statistical support. Editing and writing support was provided by A. Daisy Goodrich (Genentech, South San Francisco, CA, USA) and was funded by Genentech.

Financial support: This study was supported by Genentech, Inc., South San Francisco, CA.

T.R. Wilson, JA Ware, S. Sanabria Bohorquez, H.M. Savage, D. Sampath, L. Salphati, R.S. Lin, H. Jin, H. Parmar, and J.Y. Hsu, are employees of Genentech, Inc., South San Francisco, CA, and stock holders of Roche; I. Krop received research support from Genentech and has been a consultant for Genentech; R.K. Ramanathan received research support from Genentech; D.D. Von Hoff received research grant from Genentech to his institution for conduct of trial.

References

1. Macara IG, Marinetti GV, Balduzzi PC. Transforming protein of avian sarcoma virus UR2 is associated with phosphatidylinositol kinase activity: possible role in tumorigenesis. Proc Natl Acad Sci USA. 1984; 81:2728–32. [PubMed: 6326140]
2. Cantley LC. The phosphoinositide 3-kinase pathway. Science. 2002; 296:1655–7. [PubMed: 12040186]
3. Guertin DA, Sabatini DM. Defining the role of mTOR in cancer. Cancer Cell. 2007; 12:9–22. [PubMed: 17613433]
4. Samuels Y, Diaz LA Jr, Schmidt-Kittler O, Cummins JM, Delong L, Cheong I, et al. Mutant PIK3CA promotes cell growth and invasion of human cancer cells. Cancer Cell. 2005; 7:561–73. [PubMed: 15950905]
5. Liu P, Cheng H, Roberts TM, Zhao JJ. Targeting the phosphoinositide 3-kinase pathway in cancer. Nat Rev Drug Discov. 2009; 8:627–44. [PubMed: 19644473]
6. Ndubaku CO, Heffron TP, Staben ST, Baumgardner M, Blaquiere N, Bradley E, et al. Discovery of 2-{3-[2-(1-isopropyl-3-methyl-1H-1,2-4-triazol-5-yl)-5,6-dihydrobenzo[f]imidazo[1, 2-d] [1,4]oxazepin-9-yl]-1H-pyrazol-1-yl}-2-methylpropanamide (GDC-0032): a beta-sparing phosphoinositide 3-kinase inhibitor with high unbound exposure and robust in vivo antitumor activity. J Med Chem. 2013; 56:4597–610. [PubMed: 23662903]
7. Sahasranaman, S., Ma, S., Hsu, J., Gates, M., Ran, Y., Zhang, K., et al. Clinical Pharmacology & Therapeutics. Wiley-Blackwell; 2015. Assessment of absolute bioavailability and mass balance of the PI3K inhibitor taselisib (GDC-0032) in healthy subjects; p. S81-S.
8. Sahasranaman, S., Graham, R., Salphati, L., Hsu, J., Lu, X., Gates, M., et al. Clinical Pharmacology & Therapeutics. Wiley-Blackwell; 2015. Assessment of pharmacokinetic interaction between the PI3K inhibitor taselisib (GDC-0032) and a strond CYP3A inducer or inhibitor; p. S80-S1.
9. Graham RA, Cheeti S, Salphati L, Lu T, Kurkjian C, Von Hoff D, et al. Abstract B218: Drug-drug interaction assessment of GDC-0032, a beta-sparing inhibitor of phosphoinositide 3-kinase (PI3K), using midazolam, a sensitive CYP3A4 substrate. Mol Cancer Ther. 2013; 12:B218–B.
10. Salphati L, Wong H, Belvin M, Bradford D, Edgar KA, Prior WW, et al. Pharmacokinetic-pharmacodynamic modeling of tumor growth inhibition and biomarker modulation by the novel phosphatidylinositol 3-kinase inhibitor GDC-0941. Drug Metab Dispos. 2010; 38:1436–42. [PubMed: 20538720]

11. Salphati L, Pang J, Plise EG, Lee LB, Olivero AG, Prior WW, et al. Preclinical assessment of the absorption and disposition of the phosphatidylinositol 3-kinase/mammalian target of rapamycin inhibitor GDC-0980 and prediction of its pharmacokinetics and efficacy in human. Drug Metab Dispos. 2012; 40:1785–96. [PubMed: 22696419]
12. Pang J, Baumgardner M, Cheong J, Edgar K, Heffron TP, Le H, et al. Preclinical evaluation of the B-isoform-sparing PI3K inhibitor GDC-0032 and prediction of its human pharmacokinetics. Drug Metab Rev. 2014; 45:219.
13. Wong H, Choo EF, Alicke B, Ding X, La H, McNamara E, et al. Antitumor activity of targeted and cytotoxic agents in murine subcutaneous tumor models correlates with clinical response. Clin Cancer Res. 2012; 18:3846–55. [PubMed: 22648270]
14. Bendell JC, Rodon J, Burris HA, de Jonge M, Verweij J, Birle D, et al. Phase I, dose-escalation study of BKM120, an oral pan-Class I PI3K inhibitor, in patients with advanced solid tumors. J Clin Oncol. 2012; 30:282–90. [PubMed: 22162589]
15. Sarker D, Ang JE, Baird R, Kristeleit R, Shah K, Moreno V, et al. First-in-Human Phase I Study of Pictilisib (GDC-0941), a Potent Pan-Class I Phosphatidylinositol-3-Kinase (PI3K) Inhibitor, in Patients with Advanced Solid Tumors. Clin Cancer Res. 2015; 21:77–86. [PubMed: 25370471]
16. Ando Y, Inada-Inoue M, Mitsuma A, Yoshino T, Ohtsu A, Suenaga N, et al. Phase I dose-escalation study of buparlisib (BKM120), an oral pan-class I PI3K inhibitor, in Japanese patients with advanced solid tumors. Cancer Sci. 2014; 105:347–53. [PubMed: 24405565]
17. Gopal AK, Kahl BS, de Vos S, Wagner-Johnston ND, Schuster SJ, Jurczak WJ, et al. PI3Kdelta inhibition by idelalisib in patients with relapsed indolent lymphoma. N Engl J Med. 2014; 370:1008–18. [PubMed: 24450858]
18. Serra V, Scaltriti M, Prudkin L, Eichhorn PJ, Ibrahim YH, Chandarlapaty S, et al. PI3K inhibition results in enhanced HER signaling and acquired ERK dependency in HER2-overexpressing breast cancer. Oncogene. 2011; 30:2547–57. [PubMed: 21278786]
19. Chandarlapaty S, Sawai A, Scaltriti M, Rodrik-Outmezguine V, Grbovic-Huezo O, Serra V, et al. AKT inhibition relieves feedback suppression of receptor tyrosine kinase expression and activity. Cancer Cell. 2011; 19:58–71. [PubMed: 21215704]
20. Pratilas CA, Taylor BS, Ye Q, Viale A, Sander C, Solit DB, et al. (V600E)BRAF is associated with disabled feedback inhibition of RAF-MEK signaling and elevated transcriptional output of the pathway. Proc Natl Acad Sci USA. 2009; 106:4519–24. [PubMed: 19251651]
21. Friedman, L., Edgar, K., Song, K., Schmidt, S., Kirkpatrick, D., Phu, L., et al. The PI3K inhibitor, taselisib, has enhanced potency in PIK3CA mutant models through a unique mechanism of action. San Antonio Breast Cancer Symposium; 2016; San Antonio, TX. p. 1073Abstract S6-04Available from: https://www.sabcs.org/Portals/SABCS2016/Documents/SABCS-2016-Abstracts.pdf?v=1
22. Baselga, J., Im, SA., Iwata, H., Clemons, M., Ito, Y., Awad, aA, et al. PIK3CA status in circulating tumor DNA (ctDNA) predicts efficacy of buparlisib (BUP) plus fulvestrant (FULV) in postmenopausal women with endocrine-resistant HR+/HER2– advanced breast cancer (BC): First results from the randomized, phase III BELLE-2 trial. San Antonio Breast Cancer Symposium; 2015; San Antonio, TX. p. Abstract S6-01.
23. Leo Di, A., Keun, S., Ciruelos, E., Lønning, P., Janni, W., O'Regan, R., et al. BELLE-3: A Phase III study of buparlisib + fulvestrant in postmenopausal women with HR+, HER2-, aromatase inhibitor-treated, locally advanced or metastatic breast cancer, who progressed on or after mTOR inhibitor-based treatment. San Antonio Breast Cancer Symposium; 2016; San Antonio, TX. p. Abstract S4-07.
24. Jia S, Liu Z, Zhang S, Liu P, Zhang L, Lee SH, et al. Essential roles of PI(3)K-p110beta in cell growth, metabolism and tumorigenesis. Nature. 2008; 454:776–9. [PubMed: 18594509]
25. Juric D, Castel P, Griffith M, Griffith OL, Won HH, Ellis H, et al. Convergent loss of PTEN leads to clinical resistance to a PI(3)Kalpha inhibitor. Nature. 2015; 518:240–4. [PubMed: 25409150]
26. Mayer IA, Abramson VG, Formisano L, Balko JM, Estrada MV, Sanders ME, et al. A Phase Ib Study of Alpelisib (BYL719), a PI3Kalpha-Specific Inhibitor, with Letrozole in ER+/HER2- Metastatic Breast Cancer. Clin Cancer Res. 2017; 23:26–34. [PubMed: 27126994]
27. Spoerke JM, O'Brien C, Huw L, Koeppen H, Fridlyand J, Brachmann RK, et al. Phosphoinositide 3-kinase (PI3K) pathway alterations are associated with histologic subtypes and are predictive of

sensitivity to PI3K inhibitors in lung cancer preclinical models. Clin Cancer Res. 2012; 18:6771–83. [PubMed: 23136191]

28. Bosch A, Li Z, Bergamaschi A, Ellis H, Toska E, Prat A, et al. PI3K inhibition results in enhanced estrogen receptor function and dependence in hormone receptor-positive breast cancer. Sci Transl Med. 2015; 7:283ra51.
29. Juric D, Saura C, Cervantes A, Kurkjian C, Patel M, Sachdev J, et al. Abstract PD1-3: Ph1b study of the PI3K inhibitor GDC-0032 in combination with fulvestrant in patients with hormone receptor-positive advanced breast cancer. Cancer Research. 2013; 73:D1–3.
30. Dickler MN, Saura C, Richards DA, Krop IE, Cervantes A, Bedard PL, et al. A phase II study of the PI3K inhibitor taselisib (GDC-0032) combined with fulvestrant (F) in patients (pts) with HER2-negative (HER2-), hormone receptor-positive (HR+) advanced breast cancer (BC). J Clin Oncol. 2016; 34(suppl; abstr 520)
31. Pinheiro, J., Bates, D., DebRoy, S., Sarkar, D. the R Core Team. [cited 2017 Mar 14] nlme: Linear and Nonlinear Mixed Effects Models. R package version 3.1-131; c2017. Available from: https://CRAN.R-project.org/package=nlme
32. Eisenhauer EA, Therasse P, Bogaerts J, Schwartz LH, Sargent D, Ford R, et al. New response evaluation criteria in solid tumours: revised RECIST guideline (version 1.1). Eur J Cancer. 2009; 45:228–47. [PubMed: 19097774]
33. Faber K, Borin M, Cheeti S, Fraczkiewicz G, Nelson E, Ran Y, et al. Impact of formulation and food on taselisib (GDC-0032) bioavailability: powder-in-capsule formulation represents unique drug developmen challenge. Clin Pharmacol Ther. 2016; 99:S5–S107. [PubMed: 26803826]
34. Ding X, Faber K, Shi Y, McKnight J, Dorshorst D, Ware JA, et al. Validation and determination of taselisib, a beta-sparing phosphoinositide 3-kinase (PI3K) inhibitor, in human plasma by LC-MS/MS. J Pharm Biomed Anal. 2016; 126:117–23. [PubMed: 27187764]
35. Yan Y, Serra V, Prudkin L, Scaltriti M, Murli S, Rodriguez O, et al. Evaluation and clinical analyses of downstream targets of the Akt inhibitor GDC-0068. Clin Cancer Res. 2013; 19:6976–86. [PubMed: 24141624]
36. Arthur LM, Turnbull AK, Renshaw L, Keys J, Thomas JS, Wilson TR, et al. Changes in PIK3CA mutation status are not associated with recurrence, metastatic disease or progression in endocrine-treated breast cancer. Breast Cancer Res Treat. 2014; 147:211–9. [PubMed: 25104442]
37. Schleifman EB, Tam R, Patel R, Tsan A, Sumiyoshi T, Fu L, et al. Next generation MUT-MAP, a high-sensitivity high-throughput microfluidics chip-based mutation analysis panel. PLoS One. 2014; 9:e90761. [PubMed: 24658394]

Significance

Preliminary data consistent with preclinical data indicate increased anti-tumor activity of taselisib in patients with *PIK3CA*-mutant tumors (in comparison to patients with tumors without known activating *PIK3CA* hotspot mutations) starting at the lowest dose tested of 3 mg, thereby supporting higher potency for taselisib against *PIK3CA*-mutant tumors.

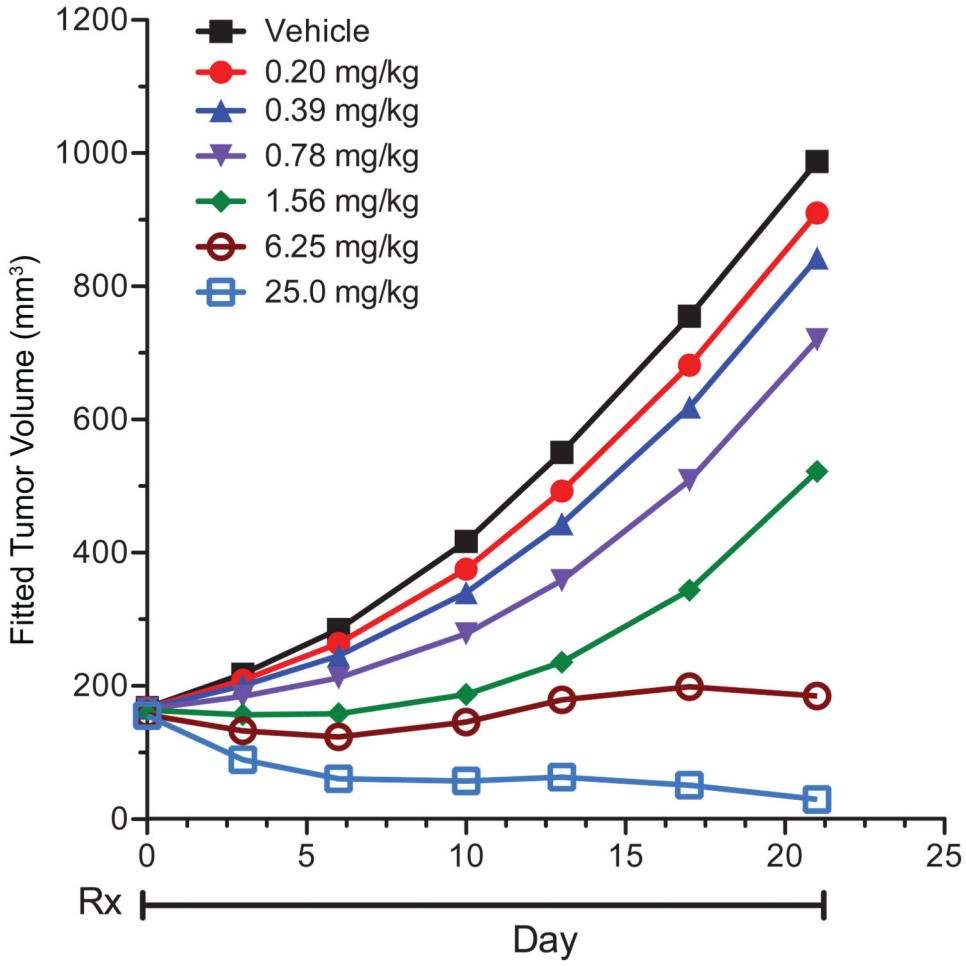

Figure 1.

In vivo efficacy of taselisib in the KPL-4 *PIK3CA*-mutant breast cancer xenograft model. Taselisib was dosed orally and daily at the doses indicated for 21 days as indicated by treatment period (Rx). Control tumor bearing mice were treated with 0.5% methylcellulose/ 0.2% Tween-80 (vehicle). Tumor volumes were measured and calculated as described in Materials and Methods.

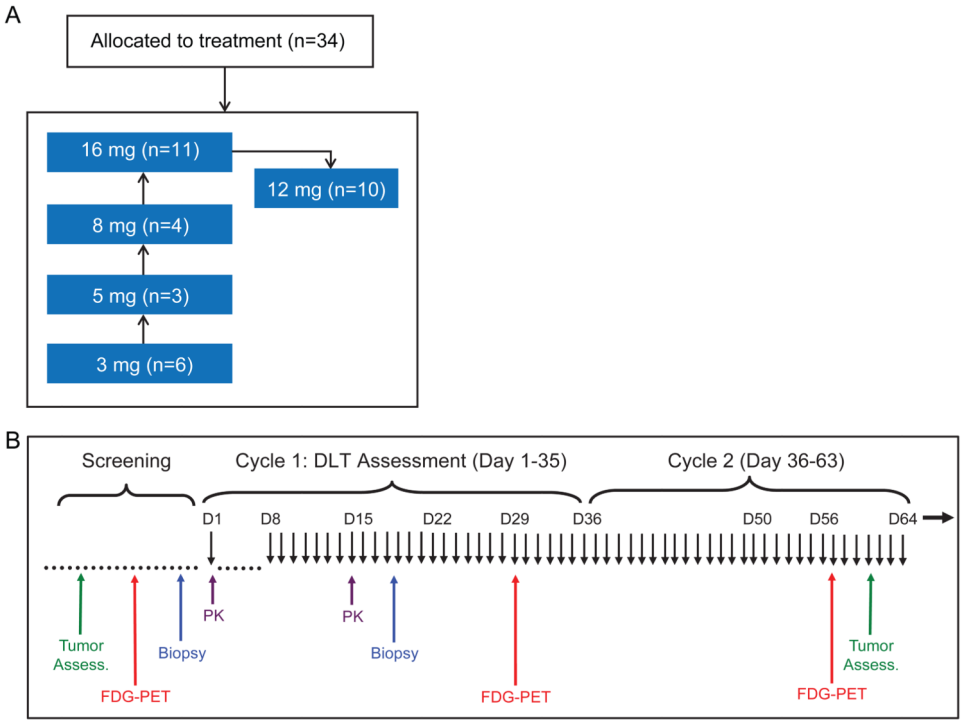

Figure 2.

Study design. (A) Phase Ia dose escalation with 5 cohort levels tested. (B) Schedule of assessments while on study.

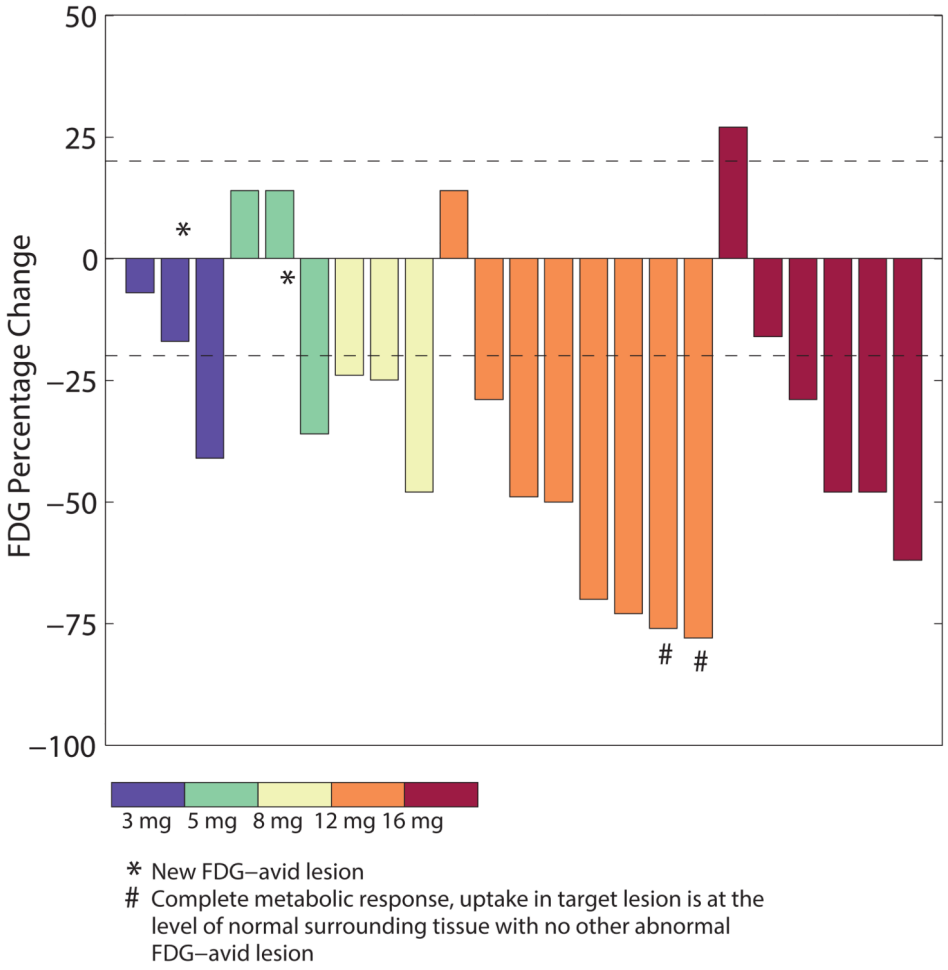

Figure 3.

Percentage change from baseline in target lesion by FDG-PET in patients in different dose cohorts.

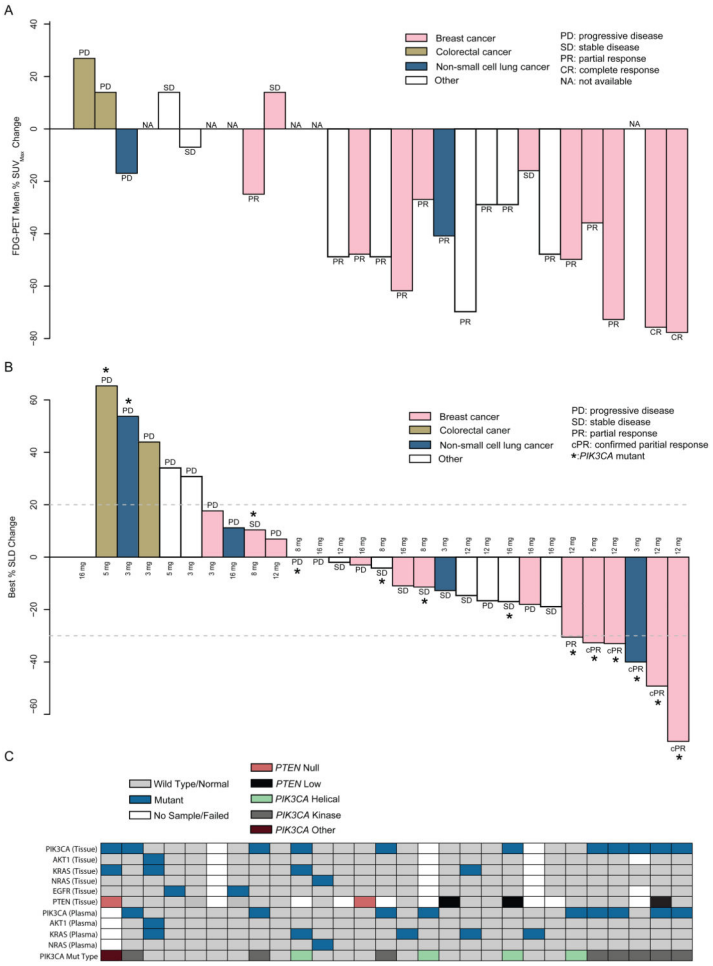

Figure 4.

(**A**) Best FDG-PET response (mean percentage change in SUV_{max}). Partial metabolic response was defined as greater than a 20% decrease in $\%\Delta SUV_{max.}$ Patients with N/A (not applicable) did not have subsequent scan after starting treatment. All patient data arranged in (**A**) are in the same patient order as in as panels (**B**) and (**C**). (**B**) Best percent change from baseline in the sum of longest diameter (SLD) for target lesions via RECIST v1.1 available for 28 measurable patients with at least one post-baseline tumor assessment for target lesion (from 29 patients with baseline measureable disease) out of 34 enrolled patients. (**C**) Corresponding somatic mutation profiling in both tumor- and plasma-extracted DNA from enrolled from patients. The patient with *PIK3CA* mutation type "*PIK3CA* Other" had an R88Q mutation.

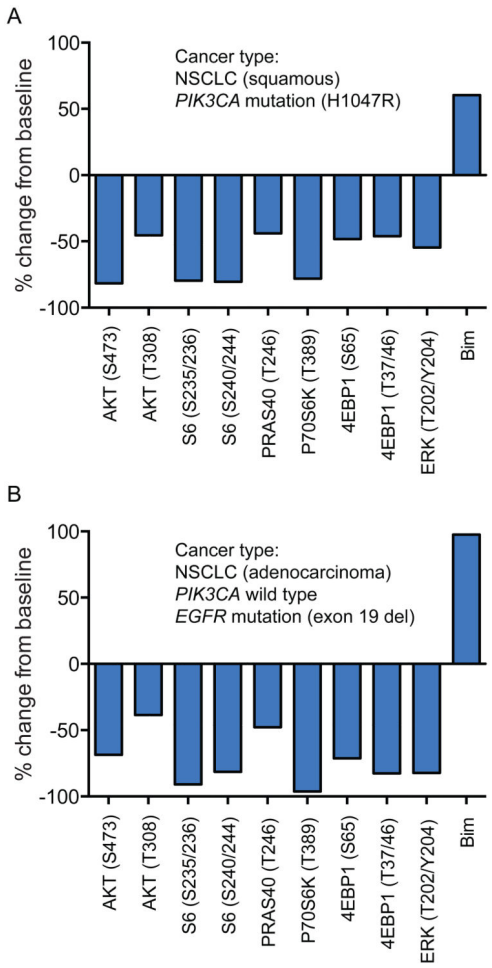

Figure 5.

Pharmacodynamic modulation of the PI3K pathway. Needle core tumor biopsies obtained from patients at baseline and at steady state (cycle 1, between days 15-21) were fixed and evaluated by reverse phase protein array for PI3K-Akt pathway markers. Decreases of > 60% in pAkt and pS6, and up-phosphorylation of BIM (pro-apoptopic protein) were demonstrated in comparison to baseline for (**A**) patient 1 on 3 mg QD taselisib with paired biopsies from right endobronchial mass and (**B**) patient 2 on 16 mg QD taselisib with paired biopsies from right upper anterior thigh mass.

Table 1

Treatment-Related Adverse Events in ≥ 5% of Patients and Adverse Events of Grade 3 or Higher

	3 mg (n=6)	5 mg (n=3)	8 mg (n=4)	12 mg (n=10)	16 mg (n=11)	All (N=34)
Adverse events in ≥ 5% of patients						
Total no. patients with ≥1 AE	6 (100%)	2 (66.7%)	3 (75%)	10 (100%)	10 (90.9%)	31 (91.2%)
Total no. AEs	17	7	7	80	115	226
Diarrhea	1 (16.7%)	1 (33.3%)	1 (25.0%)	5 (50.0%)	7 (63.6%)	15 (44.1%)
Fatigue	2 (33.3%)	1 (33.3%)	1 (25.0%)	5 (50.0%)	5 (45.5%)	14 (41.2%)
Decreased appetite	1 (16.7%)	1 (33.3%)	1 (25.0%)	5 (50.0%)	5 (45.5%)	13 (38.2%)
Hyperglycemia	0	0	2 (50.0%)	3 (30.0%)	8 (72.7%)	13 (38.2%)
Nausea	2 (33.3%)	1 (33.3%)	1 (25.0%)	3 (30.0%)	6 (54.5%)	13 (38.2%)
Stomatitis[a]	0	0	0	6 (60.0%)	4 (36.4%)	10 (29.4%)
Rash[b]	0	0	0	3 (30.0%)	3 (27.3%)	6 (17.6%)
Vomiting	0	1 (33.3%)	0	0	4 (36.4%)	5 (14.7%)
Dry Mouth	0	0	0	2 (20.0%)	1 (9.1%)	3 (8.8%)
Pruritis	0	0	0	3 (30.0%)	0	3 (8.8%)
Colitis	0	0	0	1 (10.0%)	1 (9.1%)	2 (5.9%)
Leukopenia	0	0	0	0	2 (18.2%)	2 (5.9%)
Mood altered	2 (33.3%)	0	0	0	0	2 (5.9%)
Neuropathy peripheral	1 (16.7%)	0	0	1 (10.0%)	0	2 (5.9%)
Pyrexia	0	0	0	0	2 (18.2%)	2 (5.9%)
Adverse events of ≥ grade 3						
Total no. patients with ≥1 AE	0	0	0	6 (60.0%)	8 (72.7%)	14 (41.2%)
Total no. AE	0	0	0	13	16	29
Hyperglycemia	0	0	0	2 (20.0%)	3 (27.3%)	5 (14.7%)
Rash[b]	0	0	0	3 (30.0%)	1 (9.1%)	4 (11.8%)
Diarrhea	0	0	0	0	2 (18.2%)	2 (5.9%)
Fatigue	0	0	0	0	2 (18.2%)	2 (5.9%)
Pruritus	0	0	0	2 (20.0%)	0	2 (5.9%)

	3 mg (n=6)	5 mg (n=3)	8 mg (n=4)	12 mg (n=10)	16 mg (n=11)	All (N=34)
Pneumonitis	0	0	0	0	1 (9.1%)	1 (2.9%)
Colitis	0	0	0	1 (10.0%)	0	1 (2.9%)
Exfoliative Rash	0	0	0	0	1 (9.1%)	1 (2.9%)
Lung infection	0	0	0	0	1 (9.1%)	1 (2.9%)
Renal failure acute	0	0	0	1 (10.0%)	0	1 (2.9%)
Skin exfoliation	0	0	0	0	1 (9.1%)	1 (2.9%)
Stomatitis	0	0	0	1 (10.0%)	0	1 (2.9%)

[a]Stomatitis includes the following terms: stomatitis, mucosal inflammation, lip ulceration

[b]Rash includes the following terms: rash, rash erythematous, rash maculopapular

Table 2

Pharmacokinetic Parameters of Taselisib (GDC-0032)

Cohort (Dose)	Single Dose								Steady State					
	N	C_{max} (μM)	T_{max} (hr)	$AUC_{0\text{-}24hr}$ (μM•hr)	AUC_{inf} (μM•hr)	CL/F (mL/hr)	$t_{1/2}$ (hr)	V_z/F (L)	N	C_{max} (μM)	T_{max} (hr)	C_{min} (μM)	$AUC_{0\text{-}24hr}$ (μM•hr)	CL_{ss}/F (mL/hr)
Cohort 1 (3 mg)	6	0.0256 (37%)	4 (3-8)	0.441 (32%)	1.48 (33%)	4770 (29%)	43.8 (26%)	301 (45%)	6	0.111 (65%)	3 (2-4)	0.046 (48%)	1.79 (55%)	4320 (37%)
Cohort 2 (5 mg)	3	0.0304 (40%)	8 (3-8)	0.547 (43%)	1.64 (54%)	9170 (77%)	40 (48%)	433 (39%)	3	0.091 (53%)	3 (2-4)	0.042 (55%)	1.49 (49%)	9150 (64%)
Cohort 3 (8 mg)	4	0.0764 (43%)	4 (2-4)	1.342 (34%)	3.47 (15%)	5070 (13%)	38.2 (32%)	277 (38%)	3	0.188 (63%)	3 (2-4)	0.098 (55%)	3.21 (50%)	6310 (44%)
Cohort 5 (12 mg)	10	0.127 (42%)	3 (1-8)	1.8 (35%)	4.00 (30.5%)	4750 (77%)	36.7 (20%)	267 (81%)	10	0.302 (31%)	4 (2-24)	0.128 (36%)	5.1 (40%)	4810 (61%)
Cohort 4 (16 mg)	11	0.134 (39%)	4 (2-24)	2.26 (37%)	6.36 (48%)	6640 (45%)	39.7 (20%)	372 (45%)	9	0.441 (52%)	4 (2-8)	0.241 (76%)	8.1 (57%)	5440 (61%)

$AUC_{0\text{-}24hr}$ =area under the plasma concentration-time curve from 0 to 24 hours post dose;

AUC_{inf} =area under the plasma concentration-time curve from time 0 to infinity;

CL/F =apparent clearance; $t_{1/2}$ =terminal half-life;

C_{max} =highest observed plasma concentration;

C_{min} =minimum concentration during the dosing interval;

T_{max} =time of maximum observed concentration;

V_z/F =apparent terminal phase distribution volume.

Notes: PK parameters were reported as cohort mean (%CV), except for T_{max}, which was reported as cohort median (range).